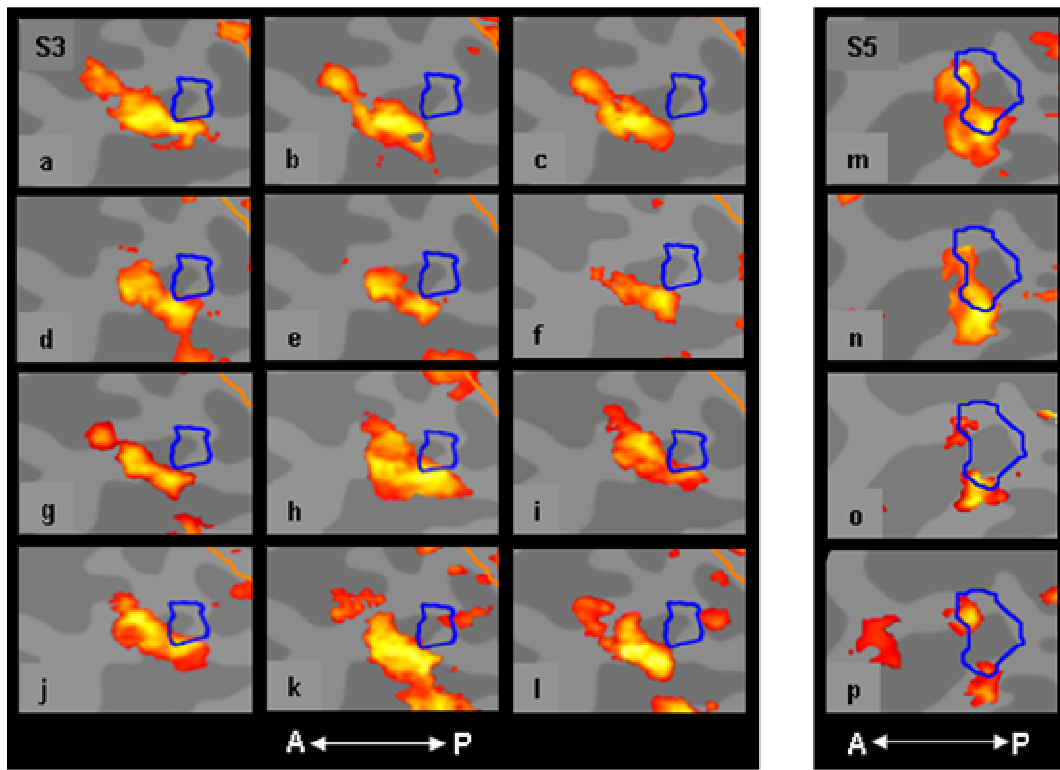


## SUPPLEMENTARY MATERIAL

### Replicability

The region of stereomotion activation had high replicability in both size and extent in different sessions run over long periods of time, as well as over a range of different presentation techniques and stereomotion rates. Examples of repeated activation are shown for two subjects on different dates. A wide range of conditions was studied in one subject in particular, including different display systems, rates, waveforms and disparity patterns. Note that the perceived trajectory of depth motion was continuous in the case of both sinusoidal and square-wave disparity modulations, even though not precisely sinusoidal for the lowest-frequency square waves. Thus, the similarity of the activation pattern is predictable from this similarity of the perceptual experience generated by the two stimulus types. Moreover, in addition to the nonius control for stable fixation, we ran control stimuli with a fixed zone of zero-disparity of dynamic noise surrounding the fixation point to further validate that vergence eye movements did not contaminate the results (Supplementary Figure 1 k, l).



**Supplementary Figure 1.** Flatmaps for two subjects (subject 3, left panel and subject 5, right panel) showing remarkable replicability of activated locations across different sessions over a period of about two years (maps constrained to the same statistical criterion as in the previous figures;  $p < 0.05$ ; color scale as in Fig. 2). The anterior-posterior axis is indicated by the A  $\longleftrightarrow$  P icons. Stereomotion activation (red-to-yellow patches) is

consistently centered anterior to the hMT+ complex (blue outline). The *left* panel illustrates the replicability in subject 3 for the main conditions CSMloc (a,c,d,f,g,l,j) and CSMdb (b,e,h) through (1) different acquisition methods and stimulus display techniques (spiral acquisition & a mirror system: a, b, c; EPI & a dichoptic AVOTEC system: the remainder); (2) continuous sine motion (d, g, j) and square-wave motion (the remainder); (3) different stereomotion alternation rates (2 Hz: f; 0.33 Hz: g; 1 Hz: the remainder); (4) with additional vergence control by a zero-disparity zone surrounding the fixation (k, l). The *right* panel shows four replications for subject 5 with partial overlap with hMT+ at 1 Hz (m) and a low temporal frequency (0.33 Hz: n), and two repetitions of the 1 Hz condition on different dates (o, p).

### Talairach Locations

The Talairach locations of the functional ROIs were quantified for the three types of motion stimuli and had standard errors of less than 3 *mm* in all cases. Specifically, the mean Talairach coordinates  $\pm 1$  s.e.m. across subjects are specified in Supplementary Table I.

**Supplementary Table I**

Stimuli		Talairach Coordinates (mm)					
		Left			Right		
		x	y	z	x	y	z
hMT+	Mean	<b>-43.6</b>	<b>-74.0</b>	<b>0.6</b>	<b>45.9</b>	<b>-68.7</b>	<b>0.3</b>
	s.d.	3.3	7.0	3.5	3.3	4.6	3.4
	s.e.m.	1.3	2.6	1.3	1.2	1.7	1.3
CSMloc	Mean	<b>-42.9</b>	<b>-65.9</b>	<b>1.1</b>	<b>44.4</b>	<b>-61.9</b>	<b>0.1</b>
	s.d.	1.9	6.3	3.8	1.8	5.3	4.9
	s.e.m.	0.7	2.4	1.4	0.7	2.0	1.9
CSMdb	Mean	<b>-43.2</b>	<b>-66.1</b>	<b>4.3</b>	<b>44.3</b>	<b>-60.4</b>	<b>3.1</b>
	s.d.	2.1	6.4	3.4	1.5	4.6	5.4
	s.e.m.	0.9	2.6	1.4	0.6	1.9	2.2

**Supplementary Table I.** Mean Talairach locations, with standard deviations (s.d.) and standard errors of the means (s.e.m.) in *mm* for the three stimulus conditions in the left and right hemispheres of the group of subjects (see also Figure 4).

The differences in Talairach localization between area centers were as follows:

for **[(CSMloc) - (hMT+)]**,

left hemisphere:  $0.7 \pm 1.8$ ,  $8.1 \pm 1.1^{**}$ ,  $0.6 \pm 1.8$ ; right hemisphere:  $-1.4 \pm 0.8$ ,  $6.9 \pm 0.7^{**}$ ,  $-0.1 \pm 2.3$  ( $n = 7$ );

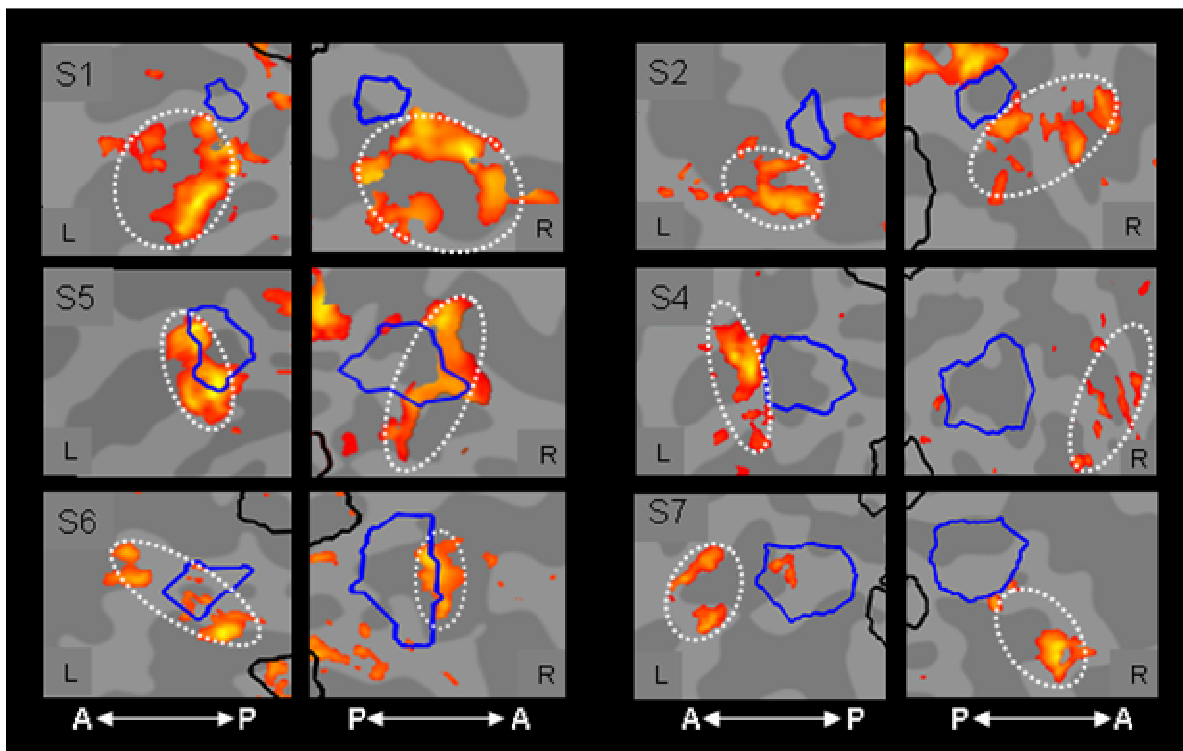
for ([CSMdb] - [hMT+]),

left hemisphere:  $0.7 \pm 1.5$ ,  $7.0 \pm 1.1^{**}$ ,  $2.8 \pm 2.2$ ; right hemisphere:  $-2.0 \pm 1.2$ ,  $8.3 \pm 1.0^{**}$ ,  $2.3 \pm 2.8$  ( $n = 6$ ).

Thus, the mean stereomotion activation was shifted significantly anterior to hMT+ in the  $y$  coordinate.

### Examples of stereomotion activation

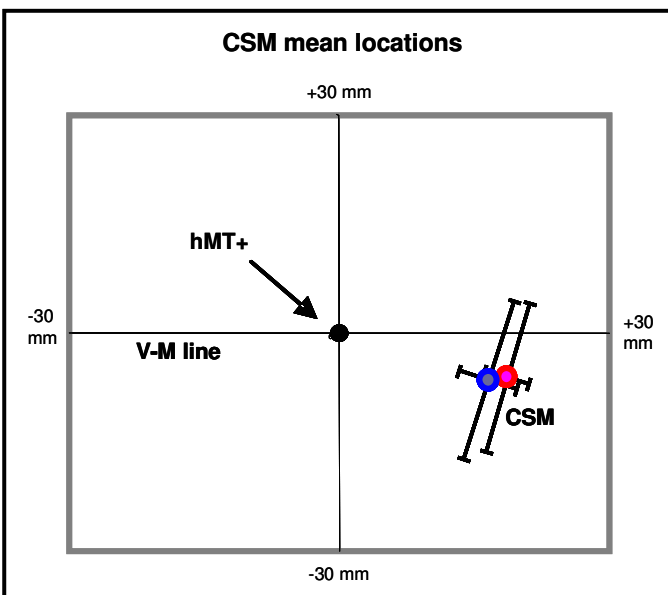
Additional examples of the stereomotion-specific activation for both hemispheres of six observers are provided in Supplementary Figure 2. This activation, roughly circumscribed by the white ellipses, is focused consistently anterior and ventral to the classic motion area (hMT+, blue outlines), with a small degree of overlap in some cases.



**Supplementary Figure 2.** Cyclopean stereomotion activations for both hemispheres (left, L; right, R) of several subjects (S) shown in flatmap format. The anterior-posterior axis is indicated by the A  $\longleftrightarrow$  P and P  $\longleftrightarrow$  A icons. Activation thresholded at a level of  $p < 0.05$ ; coherence levels color scale as in Fig. 2. Retinotopic regions V1-4 are indicated by the black outlines, identifying the posterior direction in the maps. The ROI for hMT+ is shown by the blue outline. Ellipses roughly circumscribe the CSM activations anteroventral to hMT+. Note that the significant CSM activation lies predominantly outside the hMT+ boundary. Occasional activation also appears between hMT+ and V1-4 in a few cases, but as can be seen it was not consistent among the participants.

## Flatmap Analysis

We found significant differences in Talairach coordinates along the  $y$ -axis between the hMT+ and the region activated by the stereomotion stimuli. However the stereotaxic coordinates do not fully characterize the distance between the areas through the cortical manifold due to the folded structure of the cortex. The techniques described in Methods allow us to unfold this three dimensional structure into a flat map representation and to overlay the functional activation. Therefore, to characterize the relative location of the two localizers through the cortical manifold, we first defined ROIs on flattened cortical unfolds. It should be noted, however, that the distances between pairs of specified points are then computed with an overcomplete Dijkstra algorithm (Skiena, 1990) as the minimal path between the specified locations through the voxels segmented as lying along the white/gray matter boundary. The overcomplete Dijkstra algorithm measures the true minimal distance through the undistorted cortical manifold with an accuracy of  $\pm 2.1\%$  over all directions (Schira, Tyler & Wade, in press). In addition, the angular relationships were specified on a flatmap centered on hMT+, providing a coordinate frame with no systematic angular distortions in terms of the angles between activation sites (Duncan & Boynton, 2003), although there is still a non-systematic distortion error in the optimized unfolding algorithm of less than 10%. To establish a zero for the direction axis, we define the “horizontal” direction as the line going through the center of the V1 fovea and the center of hMT+ (to be termed the V-M line). The other directions in this space are determined by the geometry of the flattening algorithm.



**Supplementary Figure 3.** The stereomotion activation (CSM) and hMT+ in a coordinate frame centered on hMT+ and oriented along the V-M line through the V1-fovea and hMT+. Both the CSMloc and CSMdb activation were centered about 2 cm from hMT+.

The corresponding experiment with balanced disparity (CSMdb) confirmed these results. The activation area was centered  $15.6 \pm 1.7^{**}$  and  $19.9 \pm 2.9^{**}$  *mm* from to the center of hMT+ in the left and right hemispheres. The measured dorsoventral displacements (in the ellipsoidal coordinate metric) of the same activations were  $-2.5 \pm 7.6$  and  $-9.5 \pm 7.4$  *mm* for CSMloc in the left and right hemispheres, respectively, and  $-6.5 \pm 5.0$  and  $-6.2 \pm 10.2$  *mm* for CSMdb, respectively, but neither of the measures deviated significantly from the V-M line or from each other, as may be seen in Supplementary Figure 2 (magenta and blue symbols, respectively). The flatmap analysis allows us to specify the mean angular directions for the CSMloc and CSMdb activations as  $13.1^\circ \pm 30.1^\circ$  and  $17.1^\circ \pm 30.4^\circ$  anterior to the center of hMT+ relative to the V-M line, respectively. In summary, the intrinsic cortical analysis shows that the distance between the stereomotion activation and hMT+ is about three times greater in intracortical distance than is implied by the mean spatial displacement in Talairach coordinates.

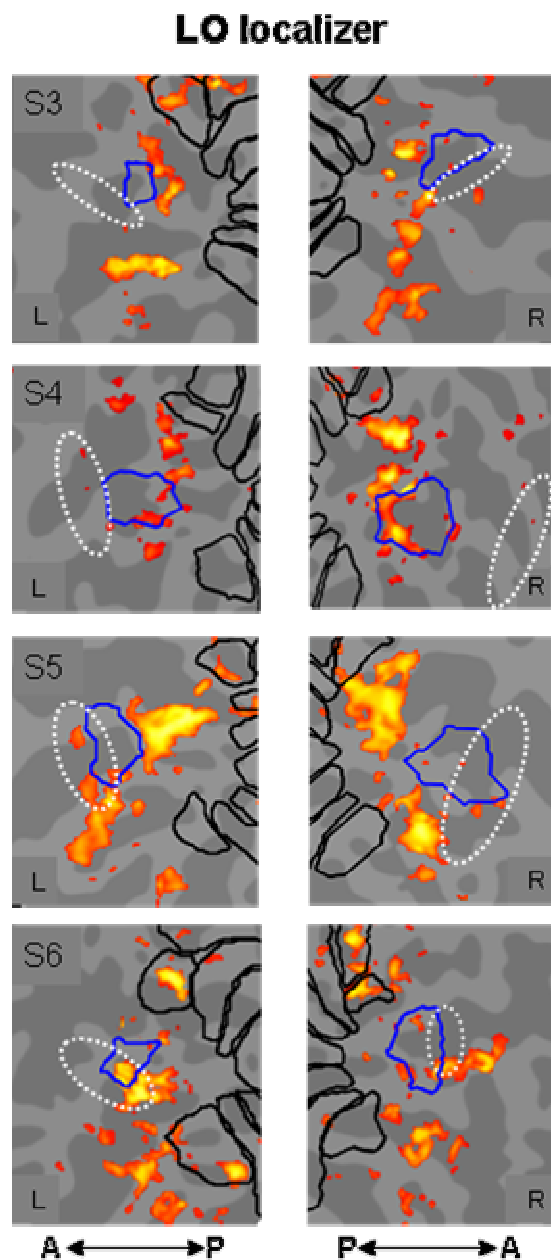
#### Does the Stereomotion Activation Overlap with the Motion Complex?

The degree of overlap between the hMT+ and the stereomotion region was quantified in three ways: the mean overlap, the number of cases in which there was no overlap, and the mean percentage of overlap in the cases of non-zero overlap. With mean left/right (L/R) hemisphere areas of  $485.6 \text{ mm}^2$  for hMT+ and  $350.4 \text{ mm}^2$  for the average of the two stereomotion areas, respectively, their mean radii in terms of a disk approximation are 12.4 and 10.6 *mm*, respectively, with a mean separation of 16 – 21 *mm*, implying a small overlap on average. In terms of the counts of overlap in activated voxels (at the significance level of  $p < 0.05$ ), there was no overlap between hMT+ and the CSMloc activation in 56% of the hemispheres studied. The area of overlap in the remaining 44% of hemispheres was only  $7\% \pm 5\%$  of the area of hMT+ on average.

#### Comparison with the lateral-occipital object area

One well-established form of activation in lateral occipital cortex is that in the lateral-occipital object (LO) area (Malach et al., 1995, 2002; Grill-Spector et al., 1998, 2001), specific to images of intact objects. To give some idea of the relationship between the locations of such object-specific activation and the CSM-specific activation of the present study, we ran a

control study for a set of LO localizer stimuli kindly provided by Zoe Kourtzi (which has been used in many fMRI laboratories such as those cited above) to identify object-specific activation



**Supplementary Figure 4.** Examples of activation (red-to-yellow: color scale as in Fig. 2) by an LO localizer (Kourtzi and Kanwisher, 2000) relative to the regions activated by the motion localizer (hMT+, blue outlines) and the general region of CSM activation (white ellipses, transferred from the previous figures). Note that the LO localizer activates a swath of cortex lying mostly between hMT+ and the retinotopic regions V1-V4 (black outlines).

This comparison consists of test stimuli depicting whole objects relative to null stimuli of spatially block-scrambled versions of the same images that contain all the same component lines, colors and local elements, but disorganized so that the objects are not recognizable. Both stimuli sets overlaid by a grid of black lines that masks the local contour breaks introduced by the scrambling.

The differential activation generated by the intact/scrambled contrast is shown for four participants in Supplementary Figure 4. It can be seen to lie mostly posterior-ventral to hMT+, showing only a small degree of overlap either with hMT+ or with the region of activation by the CSMloc stimulus, which is indicated by the white ellipses (transferred from the previous figures). These results clearly indicate that the neural network underlying stereomotion processing is functionally distinct from those for either the object-specific or luminance-based motion responses in lateral occipital cortex.